On the Initialization and Simulation of a Landfalling Hurricane Using a Variational Bogus Data Assimilation Scheme

Qingnong Xiao, Xiaolei Zou, and Bin Wang*

Department of Meteorology

Florida State University

Tallahassee, FL 32306-4520

Mon. Wea. Rev.

(submitted --- 6 January 1999)

(revised --- 24 June 1999)

(revised again --- 17 September 1999)

* Permanent affiliation: LASG, Institute of Atmospheric Physics, Chinese Academy of Sciences, Beijing 100029, China

ABSTRACT

The Bogus Data Assimilation (BDA) scheme designed to specify initial structures of tropical cyclone (Zou and Xiao 1998) was tested further on the simulation of a landfalling hurricane -- Hurricane Fran (1996). We studied the sensitivity of the simulated hurricane track and intensity to the specified radius of maximum wind of the bogus vortex, the resolution of the BDA assimilation model, and the bogus variables specified in the BDA. In addition, we compared the simulated hurricane structures with the available observations, including the surface wind analysis and the radar reflectivity captured on-shore during Fran's landfall.

The sensitivity study of the BDA scheme showed that the simulations of the hurricane track and intensity were sensitive to the size of the specified bogus vortex. Hurricanes with a larger radius of maximum sea-level pressure gradient are prone to a more westward propagation. The larger the radius, the weaker the predicted hurricane. Results of the hurricane initial structures and prediction were also sensitive to the bogus variables specified in the BDA. Fitting the model to the bogused pressure data reproduced the hurricane structure of all model variables more efficiently than when fitting it to bogused wind data. Examining the initial conditions produced by the BDA, we found that the generation and intensity of hurricane warm-core structure in the model initial state was a key factor for the hurricane intensity prediction.

Initialized with the initial conditions obtained by the BDA scheme, the model successfully simulated Hurricane Fran's landfall, the intensity change, and some inner-core structures. Verified against the surface wind analysis, the model reproduced the distribution of the maximum wind streaks reasonably well. The model-predicted reflectivity field during the landfall of Hurricane Fran resembled the observed radar reflectivity image on shore.

1. Introduction

Numerical prediction of tropical cyclone (TC) tracks has improved enormously over the past few decades, but there is little skill in forecasting the storm's intensity change (Elsberry et al. 1992) and inner-core structures (Liu et al. 1997). In fact, hurricane intensity change is closely related to the evolving three-dimensional structures of the hurricane. The difficulties in the prediction of hurricane intensity and inner core structure are associated with insufficient observations over the oceans and with the limitations of forecast models, such as low resolution, hydrostatic dynamics, crude physical parameterization and the inability to treat multiscale interactions. Recently, hurricane forecast models at high resolution have greatly improved as a result of advances in computer architecture. More sophisticated models have been developed and used for hurricane study and forecast. The Florida State University atmospheric global circulation model was run at a resolution as high as T213, which can rebuild some mesoscale signatures of the observed hurricane features with the help of satellite data using physical initialization (Krishnamurti et al. 1995). The well-known Geophysical Fluid Dynamics Laboratory (GFDL) hurricane model has been running operationally with a multiply-nested movable mesh system at a grid resolution as high as 6 km, and a very sophisticated model initialization scheme (Bender, et al. 1993; Kurihara, et al. 1995 and Ross and Kurihara 1995). The Penn State/NCAR mesoscale model MM5 was also employed to simulate the development of Hurricane Andrew of 1992 (Liu et al. 1997) and Hurricane Felix of 1995 (Zou and Xiao 1998). It was run at a grid spacing less than 10 km with explicit microphysics.

By contrast, advances in hurricane initialization have been relatively slow. With the sparse data coverage over the oceans, numerical analyses can not adequately represent the initial circulations of tropical cyclones (Leslie and Holland 1995). Hurricane initialization becomes a necessary step before making a prediction. There are several approaches for hurricane initialization: (i) substitute a specified vortex circulation defined by an analytical expression for the analyzed vortex into the initial conditions (Mathur 1991; Ueno 1989; Serrano and Unden 1994; Leslie and Holland 1995); (ii) implant a "spin-up" vortex generated by the same forecast model into the initial conditions (Kurihara et al. 1993; 1995; Peng, et al. 1993; Liu et al. 1997); and (iii) improve the initial

conditions by making use of satellite/rain gauge-based measures of rainfall through a physical initialization procedure (Krishnamurti et al. 1993; 1995; 1997; 1998). Although bogusing schemes are employed by many NWP centers, they do not always work well for a large range of tropical cyclones (Wang 1998). In order to minimize the effects of the "initial shock" resulting from the *ad hoc* assumptions in these bogus schemes, a procedure is usually needed to balance the model initial state. For example, the NCEP global model generates bogus observations, which are run through the multivariate analysis scheme. This insures that the initial state will be balanced. In the GFDL model, a quasi-balanced initial state is generated using a simplified version of the model in the bogus procedure (Kurihara et al. 1993).

In the recent work of Zou and Xiao (1998), a variational bogus data assimilation (BDA) scheme was proposed to generate the structure of a tropical hurricane in the initial condition of a high-resolution mesoscale model. In the scheme, a specified surface low based on a few observed parameters was incorporated into the model's initial conditions through a variational approach in which the forecasting model serves as a strong constraint. The initial vortex obtained by the proposed method contains a more realistic hurricane structure in all model fields and is also well-adapted to the prediction model. Such an initialization procedure is not only objective, but also flexible for the inclusion of any available observations due to its variational formulation.

The BDA scheme worked well for the numerical simulation of Hurricane Felix (1995), a hurricane which made a recurvature prior to its landfall (Zou and Xiao 1998). In this paper, we further test the performance of the BDA scheme for the numerical simulations of Hurricane Fran (1996) during its landfall, which occurred from 0000 UTC 3 September to 0600 UTC 6 September 1996. We extend the work of Zou and Xiao (1998) to examine the BDA scheme's sensitivity to model resolution, to the size of the specified vortex and to the specification of bogused SLP versus wind. The advantage of studying this case is that there were extensive observational analyses after 0000 UTC 3 September 1996 that are available from NOAA/HRD for forecast verification, such as WSR-88D radar reflectivities and surface wind analysis from before the landfall of Fran. These data are not available for Hurricane Felix (1995).

From 0000 UTC 3 September through 0600 UTC 6 September 1996, Hurricane Fran moved in a northwest direction in the western Atlantic, north of the Caribbean, and made landfall on the North Carolina coast around 0030 UTC 6 September (Figure 1). At landfall, the minimum central sea-level pressure (SLP) of Fran was estimated as 954 hPa and the maximum sustained surface winds were 51.7 m/s. The strongest winds occurred in streaks within the deep convective areas north and northeast of the center. Hurricane Fran was responsible for 34 deaths. The storm surge on the North Carolina coast destroyed or seriously damaged numerous beachfront houses. Extensive flooding caused additional damage in the Carolinas, Virginia, West Virginia, Maryland, Ohio and Pennsylvania. Fran was responsible for an estimated 3.2 billion dollars in damage to the United States (Pasch and Avila 1999).

This paper is organized as follows: The next section describes the experimental design, including a brief description of the hurricane variational initialization scheme. The BDA generated initial hurricane structure and the subsequent forecast are discussed in Sections 3 and 4. Section 5 presents the sensitivity of the forecasted hurricane's track and intensity to the size of initial vortex. The importance of bogused SLP versus wind fields in the BDA scheme is also tested in section 5. Finally, a summary and conclusions are provided in the last section.

2. Experimental Design

2.1 The Numerical Model

The numerical model used in this study is an improved version of the Penn State/NCAR nonhydrostatic, movable, triply-nested grid, 3-D mesoscale model (Dudhia 1993; Grell et al. 1994). The model consists of 27 layers in the vertical (the model top is defined at 100 hPa). The 27 half σ levels are 0.025, 0.070, 0.110, 0.150, 0.190, 0.230, 0.270, 0.310, 0.350, 0.390, 0.430, 0.470, 0.510, 0.550, 0.590, 0.630, 0.670, 0.710, 0.750, 0.790, 0.830, 0.870, 0.910, 0.945, 0.970, 0.985, 0.995. All variables except vertical velocity w are defined on the half σ levels. In the horizontal direction, the model has three nested domains A, B and C, with horizontal resolutions of 54

km, 18 *km* and 6 *km*, respectively. The coarsest domain A is fixed, but the intermediate domain B and the fine domain C moved along with the hurricane track (Figure 1). The model variables are staggered horizontally such that u and v are defined on the mid-points of all other quantities. The (x, y) dimensions are 76X85, 112X130, and 109X127 for domains A, B, and C, respectively. The time step for the coarsest domain A is 120s and complies with the 1/3 rule for the intermediate domain B and fine domain C. To reduce the computational cost, domain C is activated into integration at 66 h, when Hurricane Fran is near its landfall. We activate this fine mesh so as to obtain a more detailed hurricane structure and compare it to the observed radar reflectivity and surface winds during the landfall of Fran.

The model water cycle processes include parameterization of shallow convection for all domains, Grell (1993) cumulus parameterization and Dudhia's simple ice explicit moisture scheme for domain A, Kain-Fritsch cumulus model and Reisner mixed-phase explicit moisture scheme for domain B, and Reisner graupel explicit moisture scheme for domain C. The more sophisticated model physics was used for the higher resolution model domain. According to Zhang et al. (1988) and Molinari and Dudek (1992), convective parameterization could be bypassed for a grid size of 6 km. Other model physics include a modified version of Blackadar (1979) PBL parameterization (Zhang and Anthes 1982) and a simple radiative parameterization in which the radiation effects due to clouds are considered and calculated every twenty minutes. The SST comes from the NCEP global analysis and is kept unchanged in the model integration. However, the land surface temperature is predicted using surface energy budget equations in which the effects of short and long wave radiation and cloud radiation are included. The model also includes three-dimensional Coriolis force. Surface heat and moisture fluxes are taken into account. To deal with the acoustic waves, an upper radiative boundary condition is applied. The reader can refer to Dudhia (1993) and Grell et al. (1994) for a more detailed description of the model.

2.2 The BDA Scheme

The variational initialization scheme includes two parts. The first step is vortex specification. The second step is a minimization procedure forcing the forecast model to generate the hur-

ricane vortex. The vortex specification applies to a few model variables and the minimization procedure produces fields for all model variables, objectively satisfying the dynamic and physical constraint for the atmosphere.

a. Vortex specification

The SLP of the hurricane vortex is specified according to Fujita's formula (1952). The formula is expressed as a function of r (radial distance from the cyclone center) as follows,

$$P_o(r) = P_c + \Delta P\left\{1 - \left[1 + \frac{1}{2}\left(\frac{r}{R}\right)^2\right]^{-\frac{1}{2}}\right\} \tag{1}$$

where P_c is hurricane central pressure. ΔP is a parameter related to the hurricane SLP gradient information (which will be determined by the maximum wind as shown below). R is the estimated radius of maximum SLP gradient. The hurricane location and central pressure are specified according to the NHC observational report.

The wind can be derived from Eq. (1) in terms of the gradient wind relation, which gives

$$V_o(r) = \left(\frac{r}{\rho}\frac{\partial P_o}{\partial r} + \frac{f^2 r^2}{4}\right)^{\frac{1}{2}} - \frac{r|f|}{2} \quad . \tag{2}$$

Therefore, the hurricane maximum wind V_{max} can be calculated according to Eq. (2), and ΔP in Eq. (1) can be adjusted so as to match the observed maximum wind. ρ is air density (assumed constant). For Hurricane Fran (1996) with P_c=977 hPa and V_{max}=75 *kt* (38.8 *m/s*) at 0000 UTC 3 September 1996, the relation between ΔP and R is calculated and shown in Figure 2. In addition, there were extensive observational analyses at NOAA/HRD after 0000 UTC 3 September 1996. The radius of maximum wind (RMW) at 0000 UTC 3 September 1996 is around 80 km (marked in Fig. 2). In the vertical, the wind has a weighting profile of 1., 1., 0.95, 0.85, 0.65, and 0.35 at the corresponding 1000-, 850-, 700-, 500-, 400-, and 300-hPa levels. This vertical weighting function is

empirically determined. The gradient wind balances are not necessarily maintained at high levels before the minimization. During the minimization, model-constraint fields are then gradually produced while the BDA scheme fits the specified wind step by step.

The assigned pressure P_o and wind fields V_o values in the domain Ω are used as "observations" data to modify the MM5 analysis through a variational procedure which is described below.

b. Minimization procedure

In this procedure, a cost function is defined as

$$J(X) = J_b + J_p + J_v, \tag{3}$$

where

$$J_b = \frac{1}{2}[X - X_b]^T B^{-1}[X - X_b] \tag{4a}$$

$$J_p = \sum_{t_i}\sum_{\Omega}(P(r) - P_o(r))^T W_p(P(r) - P_o(r)) \tag{4b}$$

$$J_v = \sum_{t_i}\sum_{\Omega}\sum_{k}(V(r,k) - V_o(r,k))^T W_v(V(r,k) - V_o(r,k)) \tag{4c}$$

here $X=\{u, v, w, p', T, q\}$ represents all the model variables at the initial time. The model variables u and v are horizontal velocities, w is the vertical velocity, p' is the pressure perturbation from a constant reference state, T is the temperature and q is the specific humidity. X is gradually adjusted via an iteration procedure. X_b is the background analysis obtained from standard MM5 analysis fields with a crudely estimated diagonal error covariance matrix B. J_b represents the background term of the cost function. J_p is the pressure term, in which $P(r)$ represents the SLP of the model atmosphere. Hydrostatic relation is included in the operation to obtain the SLP from the surface pressure of the model. J_v is the wind term, in which $V(r,k)$ includes model wind velocity at sea level, 1000-, 850-, 700-, 500-, 400-, and 300-hPa level within the domain Ω. Ω is a two-dimensional domain in the vicinity of the hurricane center. The rim of Ω is defined as the limit line while SLP calculated by Eq. (1) is larger than that of the MM5 analysis. It is obvious that the area of Ω is re-

lated to R in Eq. (1). Larger R is associated with the larger area of Ω. Ω is not necessarily a circle and the average radius of Ω is about 2.5-3.5 times of R. Summation over t_i is carried out over half-hour window at every 5 minutes.

For simplicity, the background error covariance B contains only the diagonal elements. In this study, background error variances are estimated from the differences between the 12-h MM5 model forecast and the MM5 analysis at the same time. The weightings in Eq. (3), W_p and W_v, are treated as constants and determined empirically. We take W_p=1.6 $1/hPa^2$ and W_v=0.185 s^2/m^2 for all experiments (corresponding to 0.8 *hPa* pressure error and 2.325 *m/s* wind error assumed).

In order to minimize (3), a forward model and its adjoint are required. In this paper, the MM5 adjoint system (Zou et al. 1997) is used as a tool to minimize the cost function J for the purpose of obtaining the optimum hurricane initial conditions. The hurricane variational initialization is carried out on the coarsest 54-km domain (domain A) and/or the intermediate 18-km domain (domain B). The model initial conditions for the 6-*km* domains (domain C_i) are interpolated from that of the 18-*km* domain.

The dynamic structure of the MM5 adjoint system is the same as the MM5 forecast model described above. However, the physical processes that were employed in the minimization procedure are different. These processes are bulk aerodynamic planetary boundary-layer parameterization, surface friction, surface fluxes, dry convective adjustment, Kuo-type cumulus parameterization and large-scale precipitation process. The forward MM5 model and the backward adjoint version use the same set of model physics. The gradient is checked with a procedure suggested by Navon et al. (1992).

The limited-memory quasi-Newton method of Liu and Nocedal (1989) is used to minimize the objective function in this study. The background X_b (the standard MM5 analysis $X^{(0)}$) is used as the first guess of X for the minimization procedure. In all experiments, 30 iterations are performed to minimize the cost function J. After the minimization, the model fields, not only pressure and wind fields, but also temperature and humidity fields, are adjusted. The new adjusted fields are taken as the model initial conditions for the subsequent simulation.

2.3 Numerical Experiments

We conducted 9 forecast experiments for the 78-hour simulation of Hurricane Fran (1996) using the two-way interactive, triply-nested and movable mesh MM5. The differences between these experiments are in the initial conditions (listed in Table 1). CTL is the control experiment, which starts from MM5 analysis (NCEP 2.5X2.5 global analysis enhanced by rawinsondes and surface observations) without the variational initialization procedure. All other experiments use an initial condition obtained by the BDA procedure in which a bogused surface low and/or the corresponding balance wind are assimilated into the model initial conditions. These experiments differ in the horizontal resolution of the assimilation model, the size of the bogus vortex, and the bogus variables specified. Specifically, B80 is an experiment in which the BDA procedure was carried out at 18-km resolution (domain B) with 80-km RMW (radius of maximum wind). A80, A100, A140, A180, A220 and A260 are experiments in which the BDA scheme was carried out at 54 - km resolution (domain A) and with the radius R of 80, 100, 140, 180, 220 and 260 km. These experiments were designed to test the sensitivity of the hurricane forecast to the specification of the vortex size in the BDA scheme. The experiments A220P and A220V were carried out to test the relative effectiveness of SLP and wind information for the hurricane initialization and simulation. The BDA scheme in A220P minimizes J_b+J_p, and that of A220 V minimizes J_b+J_v (see Eq. (4)).

Table 1: Experimental Design

Numerical Experiment	BDA resolution (km)	bogus data (variables)	RMW (km)	Model initial Conditions
CTL				NCEP analysis
B80	18	P_o , V_o	80	BDA analyses
A80	54	P_o , V_o	80	
A100	54	P_o , V_o	100	
A140	54	P_o , V_o	140	
A180	54	P_o , V_o	180	
A220	54	P_o , V_o	220	
A260	54	P_o , V_o	260	
A220P	54	P_o	220	
A220V	54	V_o	220	

3. Results from BDA Scheme

3.1 Efficiency of the Technique

We performed 30 iterations of the minimization procedures in all the BDA experiments. Figure 3 shows the variations of the three terms in the cost function, J_b, J_p and J_v, during the 30 iterations for B80. The performance of the minimization for the other experiments was similar. As expected, the pressure and wind terms decreased at the expense of the background term increase. Since X_b is used as the initial point of the minimization, the background term is equal to zero at the beginning of the minimization and increases with the number of iterations. The figure indicates that the minimization converged very quickly in the first 5 iterations. After the background term was increased to a value close to the "observational" terms, the adjustment in the model's initial condition became smaller. Usually 15 iterations were enough to obtain the optimal initial condition with a reasonable accuracy.

To show the effectiveness of the BDA minimization procedure, Table 2 lists values of the central SLP and the low-level maximum wind of the initial vortex in all the experiments. The ob-

served hurricane central pressure and maximum wind are also listed in table 2. We can see that the BDA technique was, in general, capable of producing an initial hurricane with an intensity very close to the observed value. The central SLP of the hurricane center was 1008 hPa from the standard MM5 analysis. After the BDA procedures, the SLP decreased at least 20 hPa for all the experiments except A220V. The observed low-level maximum wind reached 38.8 m/s, while the MM5 standard analysis was only 15.0 m/s. After BDA, the low-level maximum winds increased by at least 20 m/s for all the variational experiments. We thus notice that the assimilation of the specified SLP adjusted the wind field to a great extent, but the assimilation of the bogused wind data alone did not make significant changes in the SLP field. The proposed BDA scheme is quite robust with respect to the specifications of the vortex size and has great skill in reproducing the observed initial hurricane intensity. An additional advantage of the BDA scheme is its ability to produce dynamically and physically consistent hurricane structures of *all* model fields, which are shown in the following sub-section.

Table 2: Hurricane central SLP and low-level maximum wind speed for all the initialization experiments

	OBS	CTL	B80	A80	A100	A140	A180	A220	A260	A220P	A220V
CSLP (hPa)	977	1008	977	982	980	978	978	978	982	976	1006
V-Max (m/s)	38.8	15.0	37.7	36.5	37.5	37.7	37.3	37.5	36.6	26.1	34.6

CSLP represents the central SLP and V-Max is the low-level maximum wind speed.

3.2 The Thermodynamic Structure of the Initial Hurricane obtained by B80

During the BDA procedure, the temperature and humidity fields are also modified so as to balance the pressure and wind adjustment within the hurricane area. Figure 4 shows the cross-section of the temperature and humidity fields before and after the initialization in experiment B80. It can be seen that the NCEP analysis (Figure 4a, b) lacked the structure that a mature hurricane has in the temperature and humidity fields. The temperature and humidity contours were flat above the cyclone. Since there are few, or no, radiosonde observations over the open ocean, the hurricane

temperature and humidity fields were nearly the same as the environmental fields in the global analysis (Figure 4a). After BDA, the hurricane temperature and humidity fields were modified and the temperature above the hurricane center increased (Figure 4c). In the lower troposphere, the water vapor content also increased (Figure 4d). The temperature and moisture structures in Figures 4c and 4d indicate a mature hurricane structure with a warm, moist core. However, in the BDA scheme, surface temperature is not a control variable. It is, therefore, not adjusted after the initialization. That is why the lower air temperature in the eye is much greater than the sea-surface temperature (SST). Further work is needed to incorporate surface temperature into the BDA scheme to overcome this unrealistic feature.

The shaded areas in Figures 4c and d are the BDA analysis increments of the temperature and specific humidity. The temperature increases are as large as 6°C at 700-*hPa* and 200-*hPa*. The maximum increase in the humidity field occurred in the lower troposphere above the hurricane center (Figure 4d), with a 6 g/kg increase observed near 850 *hPa* and 700 *hPa*. Such an adjustment in the temperature and specific humidity are a result of the model's fit to the bogus data constraint. There was no direct information on the temperature and specific humidity in the bogus data and no structure function in the background term. The hurricane warm-core structure was formed with the use of the BDA scheme. Moisture increase in the lower troposphere is very important for hurricane development (Liu et al. 1997). Such a modification will facilitate the triggering of deep convection associated with the storm and reduce the spin-up problem of model integration.

4. Experimental Results from the Simulation of Hurricane Fran (1996)

According to the real-time surface wind analyses prepared by HRD/AOML/NOAA (Hurricane Research Division, Atlantic Oceanographic and Meteorological Laboratory, National Oceanic and Atmospheric Administration), Hurricane Fran had a radius of maximum wind (RMW) close to 80 km at 0000 UTC 3 September 1996. Two experiments, A80 and B80, which both had a RMW of 80 km (close to the observed one), were carried out to examine the performance of the BDA scheme on the initialization and simulation of the landfall of Hurricane Fran while studying

the sensitivities of the numerical results to the horizontal resolution of the assimilation model used in BDA.

Figure 5 shows the predicted hurricane tracks of Fran (1996) from CTL, A80, and B80, starting from 0000 UTC 3 September 1996. The NHC observed best track (OBS) is also plotted for comparison. Starting from 0000 UTC 3 September, the observed storm moved north-northwestward and landed at about 0030 UTC 6 September on the North Carolina coast. The CTL simulated hurricane track is on the west side of the observed track and the position error at 78 h is about 352 km (see also Table 3). The landing time predicted by CTL had a 6-h delay. On the contrary, the hurricane tracks from A80 and B80 were on the east side of the observed track. The errors in both the movement and landing time were much reduced (Fig. 5 and Table 3). At 78 h of model integration, the track forecast made by B80 has about 96.5 km position error. The forecasted landing time was about 1 hour earlier than the observed one. This demonstrates the positive impact of the BDA scheme on the hurricane track prediction.

Table 3: Hurricane track errors for A80, B80 and CTL (km)

EXP.	6h	12h	18h	24h	30h	36h	42h	48h	54h	60h	66h	72h	78h
CTL	107.1	155.6	153.2	52.7	108.3	172.6	132.4	183.5	200.2	320.8	347.2	339.2	352.7
A80	34.5	175.6	84.3	64.8	65.8	58.6	75.3	129.1	157.6	172.0	198.2	196.5	170.4
B80	7.5	77.5	83.2	7.0	12.5	24.7	60.2	82.2	90.2	97.7	123.9	110.5	96.5

The hurricane track predicted by A80 with the BDA scheme carried out on 54-km resolution (domain A) was slightly degraded. The simulated track was further to the east and slightly faster than that of B80.

Figure 6 depicts the time variation of the minimum central pressure (Figure 6a) and the maximum low-level winds (Figure 6b) from CTL, B80, and A80. The observed minimum central pressures and the maximum low-level winds from observations are also shown as a reference in the figure. The simulated maximum low-level wind is the highest value of the averaged 25th and 26th model level winds calculated at each grid point. Without the variational initialization procedure, model simulation (CTL) did not capture the intensity of Hurricane Fran, either in the central

pressure or the maximum low-level winds. The errors from B80 and A80 simulations initialized with the BDA technique were significantly smaller compared to CTL. The spin-up problem seen during the first 6-h integration of A80 and B80, reflected in the central pressure jump during that interval in Fig. 6a, is probably due to the use of triply-nested domains for predication and a single domain for initialization.

According to the HRD real-time surface wind analysis and NHC aircraft reconnaissance (Pasch and Avila 1999), Hurricane Fran had its maximum wind streak from the east to the north-northeast of the hurricane center. Figure 7 shows the surface analyses of the streamlines and isotachs (kt) at 0100 and 0700 UTC 5 September 1996 using the available observations and the aircraft reconnaissance by HRD/NOAA. The maximum winds are observed to the northeast of the hurricane center. The maximum surface wind at 0100 UTC is 95 kts (49.1 m/s). It is 90 kts (46.5 m/s) at 0700 UTC 5 September 1996. The simulations of the hurricane surface wind fields at 0100 and 0700 UTC 5 September 1996 are shown in Fig. 8 a and b, respectively. We can see that the simulated maximum wind streaks were located in the north-east quadrant. The maximum surface wind was 49.6 m/s at 0000 UTC 5 September and 56.3 m/s at 0600 UTC 5 September 1999. The simulated wind features resemble the HRD real-time surface wind analysis. However, the simulated RMW is slightly smaller than the observations.

To show the structures of the simulated Hurricane Fran, the vertical cross-sections of temperature, specific humidity, horizontal wind and vertical velocity of the B80 simulated 49-h hurricane along line AB in figure 8a are given in Figure 9. The temperature field had an evident warm core above the hurricane (Figure 9a) because of compensating descent inside the hurricane eye. The maximum value of specific humidity occurred near the surface in the hurricane center (Fig. 9b). The regions of maximum moisture were in the eye walls from lower to middle troposphere. The hurricane center area was not as moist as the eyewall regions from 600 hPa to 950 hPa. As seen in Figure 8a, the cross-sections are along the direction of the most asymmetric wind. Therefore, the wind fields in Figure 9c also depict the asymmetric characteristics in the vertical distribution. The radius of the maximum wind increases with the height. It is noted that the ascending

motion (Figure 9d) was also not axi-symmetric. The axes of the ascending motion in the eyewall and the compensating descent in the hurricane eye were tilted. The maximum ascending vertical motion occurred between 400-500 hPa in the eyewall.

From the simulated results we can summarize the following characteristics of the hurricane's flow and its thermodynamic structure. 1) The tangential or swirling wind of the hurricane is strongly asymmetric. The maximum wind speed occurred around 900 hPa. 2) The ascending vertical motion around the eye increases the moisture in that region, while the descent inside the eye makes the area of the hurricane center drier in the lower to middle troposphere. Near the surface at the hurricane center, the specific humidity reaches its maximum value. 3) The compensating descent inside the hurricane eye is the main reason for the formation of the warm core. Because the temperature increase does not occur in the eyewall where the convective latent heating release takes place, we suspect that convective latent heating release is not the main reason for the formation of the hurricane's warm core.

At 66 h of model integration, the 6-km grid-spacing domain C was activated. Therefore, we obtain a detailed hurricane forecast structure which can be compared with the on-shore radar reflectivity distribution observed during the landfall of Hurricane Fran. The radar reflectivity was estimated from the model cloud water, rain water and other ice particles such as graupel. The method for calculation of the model reflectivity was the same as that in Liu et al. (1997) and it was based on the R-Z relation of Jorgenson and Wills (1982) and Fujiyoshi et al. (1990). Contributions of cloud water to reflectivity were small and therefore neglected. For Hurricane Fran, the structure of the storm at landfall was well captured by the WSR-88D radar on shore at North Carolina (Fig. 10b). The radar-observed stronger reflectivity represents the deep convection that occurred in the north-northwest area of the hurricane center. The simulated reflectivities of Hurricane Fran immediately after its landfall (Figure 10a) showed that the simulated strong reflectivities were also in the north-northwest section of the hurricane center. The model reproduced very well the intense precipitation in the north-northwestern direction of the hurricane center, in accordance with the radar observations on shore. The horizontal structure of radar reflectivities were highly asymmetric

from both the simulation and observation. The simulated higher radar reflectivities were more intense over land, a feature consistent with observations from the on-shore radar at 0028 UTC 6 September 1996.

It must be pointed out that the simulation of B80 has some shortcomings. The predicted hurricane intensity is still weak compared with observation. The spin-up problem is not eliminated during the first 6-h integration. The simulated winds in the hurricane environment are weaker than the analysis from observations (compared Fig. 7 with Fig. 8). It is necessary to conduct more experiments and case studies to improve the BDA scheme in the future.

5. Sensitivities of the BDA results to the model resolution, RMW and bogus variable specification

The specification of the bogus vortex (see Eq. (1)) requires knowledge of the RMW. The RMW is not always known, nor can it be estimated exactly. Previous studies, such as Fiorino and Elsberry (1989), addressed the sensitivity of hurricane prediction to the RMW using barotropic models. In our study, however, the baroclinic effects were included through the use of the primitive-equation mesoscale model MM5. We will examine the influence of the specified RMW upon the prediction of hurricane track and intensity using BDA. In addition, we will also test the relative importance of specifying the bogused SLP versus wind in the BDA scheme for the hurricane initialization and prediction.

5.1 Influence of the model resolution and specified vortex RMW in BDA

Figure 11 gives the predicted hurricane tracks of Fran (1996) for a set of experiments CTL, A80, A100, A140, A180, A220 and A260, all initialized at 0000 UTC 3 September 1996. All the experiments initialized with the BDA scheme produced hurricane tracks east of the observed track, except in the beginning 6 hours of the model integration. The results show that the predicted hurricane track is sensitive to the specified RMW, i.e., R in Eq. (1). For RMW greater than 100 km, the storm moved more westward with time as the radius increased. This is shown more clearly for

the tracks beyond 48 h. This numerical result is consistent with the result of barotropic model simulation by Fiorino and Elsberry (1989). The baroclinic effects included in MM5 did not change the propagation tendency. However, the track predicted by A80 is more westward than those predicted by A100 and A140. We suspect that the 54-km grid-spacing is not sufficient to resolve the initial hurricane structure with a 80-km RMW hurricane.

Figure 12 depicts the time variation of the minimum central SLP (Figure 12a) and the maximum low-level winds (Figure 12b) from simulations with different values of RMW. All the forecasts initialized with the BDA procedure matched Hurricane Fran's intensity change well. The intensifying period from 0 to 48 h and weakening period after 48 h were predicted. However, the hurricane intensity forecast was sensitive to the specified RMW. For RMW larger than 100 km, the hurricane weakens as the RMW increases. An exception occurred to A80 for the reasons mentioned above. With BDA being carried out at 54-km resolution and RMW being equal to 180 km and 220 km, the forecasts performed better than the other experiments for both the hurricane track and intensity simulations. Their forecast performances are comparable to B80. In summary, both A180 and A220 simulated an intensity and intensity variation very close to the observed one, although these two experiments were done at the resolution of 54-km (instead of 18 km) and the RMW used in the BDA was larger than the observed one.

5.2 Relative Importance of SLP Versus Wind Information in Specifying the Initial Vortex

The BDA experiments described above include two types of bogus data: the SLP and wind. In this section, we perform two additional experiments, one without the bogused wind (A220P) and the other without the bogused SLP (A220V). The BDA schemes of both experiments were performed at 54-km resolution (domain A) and the RMW was taken as 220 km, because A220 produced reasonably good simulations in both the hurricane track and intensity. We are interested in seeking an answer to the question: which type of bogused data is more important for the hurricane initialization and forecast using the variational approach?

Figure 13a presents the hurricane SLP and 850 hPa wind field after minimization of

A220V. The pressure field after the BDA with bogused winds alone (Fig. 13a) is still weak and does not match well with the wind fields. The surface low was extended to the northeast compared to the NCEP global analysis (Fig. 13c), but the center was still located about 50 km southwest of the hurricane wind circulation (vortex). Only a 2 hPa change occurred to the central pressure value through the assimilation of wind data in A220V. In A220P (Figure 13b), not only the bogused pressure field was assimilated into the model's initial condition, but also the wind fields were significantly adjusted, showing a more compact, asymmetric distribution compared to the NCEP global large-scale analysis (see Fig. 13c). The maximum 850-hPa wind was in the north-eastern quadrant of the hurricane cyclone, the same as that observed in B80. We notice that the BDA generated pressure and wind fields in Figures 13a (and 13b to some extent) do not necessarily satisfy the balance equation. The complete forecast model serves as the dynamic and physical constraint in the BDA scheme.

Figure 14 shows the predicted hurricane intensity variations of A220P and A220V for the 78-h simulations. As a comparison, the intensity changes of A220 and the NHC observations are also shown in Figure 14, along with A220P and A220V. At the initial time, A220P had a hurricane central pressure of 976-hPa and a maximum low-level wind of 26.1 m/s, while in A220V the central pressure was 1007-hPa and the maximum low-level wind was 34.6 m/s. This implies that the assimilation of the bogused wind alone could not produce a hurricane SLP field with realistic intensity. On the contrary, the wind fields were significantly adjusted while assimilating the bogused SLP data. The subsequent 78-h model simulations show that A220V predicted a relatively weaker hurricane, although the forecasting skill in A220V is improved compared to CTL. The predicted hurricane central pressure and low-level maximum wind speed at 54 h were 982 hPa and 42 m/s, respectively. It is interesting to note that, although the low-level maximum wind of A220V at the beginning was very close to the observation, the forecast became poorer as the time of integration increased. A precise specification of wind fields alone in the BDA scheme seems insufficient to obtain a prediction with a realistic intensity and intensity change if no related pressure field is also specified in the scheme. A220P had an overall better performance than A220V, although the wind

fields at the initial time were slightly weaker and the model prediction suffered a 12-h spin-up problem (Figure 14a,b). It should be pointed out that the predicted hurricane low-level maximum winds in A220P were closer to the observation than in A220V, although the wind was not bogused into the model initial condition in A220P. From these experiments, we conclude that the pressure bogus is more efficient than the wind bogus in reproducing a realistic hurricane intensity forecast. This reconfirms the importance of the surface low information in the pressure field for the hurricane BDA initialization (Zou and Xiao, 1999).

Figure 15 shows the adjustments of the temperature and humidity fields of A220P and A220V. The warm and moist core in the initial vortex of A220P (Figures 15c, d), is not produced in the initial vortex of A220V (Figures 15a, b). The temperature fields in Figure 15a were similar to the CTL experiment (Figure 4a). In A220P, however, the warm core is stronger than that in A220 (Figure omitted). This may be part of the reason that A220P produced a stronger hurricane intensity forecast compared to A220. The stronger initial warm core in A220P resulted in a deeper hurricane central pressure in the model simulation, and hence intensified the hurricane circulation (wind fields). Because no warm-core was formed at the initial time in A220V, the simulated hurricane intensity was too weak.

The above two experiments indicate that the pressure field is more important than the wind field in generating hurricane structure using BDA. With the cost function (4b) included, the wind field is adjusted to keep (4b) small and force the pressure and wind field to a balanced state. Otherwise, the pressure field will change very rapidly during the model integration and the cost function (4b) may not be minimized. Although tropical cyclogenesis is emphatically not a simple process, our results from the BDA experiments indicate that collecting more information for formulating the bogused SLP field is effective in generating initial structures of a mature hurricane using the BDA technique. However, both pressure and wind observation data are necessary to obtain a better forecast, as is clearly shown from the results of this study. Ideally speaking, rotationally balanced wind and pressure vortex fields should be used as the data constraints in the assimilation. Then, the divergent circulation in the vortex will be generated during the data assim-

ilation with a thermally active prediction model.

6. Summary and Conclusions

One of the most challenging problems for the tropical cyclone forecaster and researcher is defining the structure of the tropical cyclone and the adjacent synoptic features with insufficient observations over the ocean. In this paper, the BDA scheme for hurricane initialization, proposed by Zou and Xiao (1999), is tested for the landfalling simulation of Hurricane Fran (1996). We studied the sensitivity of the BDA scheme to the model resolution, the radii of maximum SLP gradient for the specification of the bogus vortex, and the type of bogus data assimilated in the BDA. Numerical simulations of MM5 using the BDA scheme showed a remarkable forecast skill in reproducing the movement, intensity, and structure of Hurricane Fran near landfall. Sensitivity studies reveal many interesting features. The most important results are summarized as follows:

- The BDA scheme is very efficient in recovering the initial structure of the hurricane using very little observational information. Because the hurricane forecast model was used as a strong constraint in the hurricane BDA scheme, all model fields were adjusted to fit the bogus data of the SLP low and the derived balance wind fields. For instance, a moist warm-core hurricane structure was found in the initial vortex after BDA. These are adjustments in the model variables not directly bogused. An automatic result of BDA is that the initial conditions were consistent with the hurricane forecast model.

- The simulation of the hurricane track was sensitive to the model resolution on which the BDA scheme was performed. The predicted hurricane track was improved from the initialization with higher resolution. But the improvement from using higher resolution does not occur in the intensity forecast.

- In the present case with the current model configuration, the RMW used in the BDA scheme is a sensitive parameter for the hurricane track and intensity forecast. If the selected domain grid mesh can resolve the specified bogus vortex, hurricanes with larger RMW have a larger component of westward motion and are usually weaker.

• The sensitivity study shows that assimilation with the use of the bogused SLP field in the BDA scheme is more effective than the wind fields in recovering hurricane structure in all model variables. The hurricane simulation from the initial conditions produced by the use of bogused SLP low data is closer to observation than the use of bogused wind data only.

• Despite the differences resulting from variations in bogus data and model resolution, all the forecast experiments initialized with the BDA scheme obtained reasonably good hurricane track forecasts, which were reflected in the landfall location and the landfalling time. It is of particular importance that the BDA scheme showed great capabilities in reproducing the intensity and intensity changes of Hurricane Fran.

• The hurricane flow structure is simulated well using BDA and is in conformity with the structures illustrated by many authors such as Willoughby (1995). During the landing period of Fran, the model-simulated wind and reflectivity exhibited many structures similar to the observed wind and radar reflectivity distributions on shore.

This study is a natural extension of the work by Zou and Xiao (1999) where the BDA scheme was tested for the prediction of Hurricane Felix (1995). It is demonstrated that the BDA scheme works well, not only for a developing hurricane, but also for a mature hurricane simulation. The studies of the sensitivity of the BDA scheme to the model resolution, the RMW of the specified bogused SLP low, and the bogus variables in BDA, increased our understanding of the performance of the BDA scheme in many aspects. Further experiments will be conducted to assess the capability, propriety and feasibility of the proposed scheme for operational application.

Acknowledgments: This research has been supported by AFSOR under grant F4920-96-C-0020 and ONR under grant N00014-99-1-0022. Thanks to Drs. Z. Zhang at the Florida State University and L. Wu at the University of Hawaii for many helpful discussions. Thanks also to Dr. Y. Liu of McGill University for providing the diagnosis software for model radar reflectivity calculation. The authors gratefully acknowledge the Mesoscale and Microscale Meteorology Division (MMM) and Scientific Computing Division (SCD), National Center for Atmospheric Research (NCAR) for

providing computing time on Cray machines.

References

Bender, M. A., R. J. Ross, R. E. Tuleya, and Y. Kurihara, 1993: Improvements in tropical cyclone track and intensity forecasts using the GFDL initialization system. *Mon. Wea. Rev.*, **121**, 2046-2061.

Dudhia, J., 1993: A nonhydrostatic version of the Penn State-NCAR mesoscale model: Validation tests and simulation of an Atlantic cyclone and cold front. *Mon. Wea. Rev.*, **121**, 1493-1513.

Elsberry, R. L., K. A. Emanuel, G. Holland, H. Gerrish, M. DeMaria, and C. Guard, 1992: Is there any hope for tropical cyclone intensity prediction? A panel discussion. *Bull. Amer. Meteor. Soc.*, **73**, 264-275.

Fiorino, M., and R. L. Elsberry, 1989: Some aspects of vortex structure related to tropical cyclone motion. *J. Atmos. Sci.*, **46**, 975-990.

Fujita, T., 1952: Pressure distribution within a typhoon. *Geophys. Mag.*, **23**, 437-451.

Fujiyoshi, Y., T. Endoh, T. Yamada, K. Tsuboki, Y. Tachibana, and G. Wakahana, 1990: Determination of a Z-R relationship for snowfall using a radar and high sensitivity snow gauges. *J. Appl. Meteor.*, **29**, 147-152.

Grell, G. A., 1993: Prognostic evaluation of assumptions used by cumulus parameterization. *Mon. Wea. Rev.*, **121**, 764-787.

Grell, G. A., J. Dudhia, and D. R. Stauffer, 1994: A description of the fifth generation Penn State/ NCAR mesoscale model (MM5). *NCAR Tech Note*, NCAR/TN-398+STR, 138pp.

Jorgenson, D. P., and P. T. Wills, 1982: A Z-R relationship for hurricanes. *J. Appl., Meteor.*, **21**, 356-366.

Krishnamurti, T. N., H. S. Bedi, and K. Ingles, 1993: Physical initialization using SSM/I rain rates.

Tellus, **45A**, 247-269.

Krishnamurti, T. N., S. K. Roy Bhowmik, D. Oosterhof, and G. Rohaly, 1995: Mesoscale signatures within the tropics generated by physical initialization. *Mon. Wea. Rev.*, **123**, 2771-2790.

Krishnamurti, T. N., R. Correa-Torres, G. Rohaly, and D. Oosterhof, 1997: Physical initialization and hurricane ensemble forecasts. *Weather and Forecasting*, **12**, 503-514.

Krishnamurti, T. N., W. Han, B. Jha, H. S. Bedi, 1998: Numerical prediction of hurricane Opal. *Mon. Wea. Rev.*, **126**, 1347-1363.

Kurihara, Y., and R. J. Ross, 1993: An initialization scheme of hurricane models by vortex specification. *Mon. Wea. Rev.*, **121**, 2030-2045.

Kurihara, Y., M. A. Bender, R. E. Tuleya, and R. J. Ross, 1995: Improvements in the GFDL hurricane prediction system. *Mon. Wea. Rev.*, **123**, 2791-2801.

Lislie, L. M., and G. J. Holland, 1995: On the bogusing of tropical cyclones in numerical models: A comparison of vortex profiles. *Meteorol. Atmos. Phys.*, **56**, 101-100.

Liu, D. C., and J. Nocedal, 1989: On the limited memory BFGS method for large scale optimization. *Mathematical Programming*, **45**, 503-528.

Liu, Y., D.-L. Zhang and M. K. Yau, 1997: A multiscale study of Hurricane Andrew (1992). Part I: Explicit simulation and verification. *Mon. Wea. Rev.*, **125**, 3073-3093.

Mathur, M. B., 1991: The National Meteorological Center's quasi-Lagrangian model for hurricane prediction. *Mon. Wea. Rev.*, **109**, 1419-1447.

Molinari, J., and M. Dudeck, 1992: Parameterization of convective precipitation in mesoscale numerical models: A critical review. *Mon. Wea. Rev.*, **120**, 326-344.

Navon, I. M., X. Zou, J. Derber, and J. Sela, 1992: Variational data assimilation with an adiabatic version of the NMC spectral model. *Mon. Wea. Rev.*, **120**, 1433-1446.

Pasch, R. J., and L. A. Avila, 1999: Atlantic hurricane season of 1996. *Mon. Wea. Rev.*, **127**, 581-610.

Peng, M. S., B.-F., Jeng, C.-P. Chang, 1993: Forecast of typhoon motion in the vicinity of Taiwan

during 1989-90 using a dynamical model. *Weather and Forecasting*, **8**, 309-325.

Ross, R. J., and Y. Kurihara, 1995: A numerical study on influences of Hurricane Gloria (1985) on the environment. *Mon. Wea. Rev.*, **123**, 332-346.

Serrano, E., and P. Unden, 1994: Evaluation of a tropical cyclone bogusing method in data assimilation and forecasting. *Mon. Wea. Rev.*, **122**, 1523-1547.

Ueno, M., 1989: Operational bogussing and numerical prediction of Typhoon in JMA. *JMA/NPD Technical Report,* **No. 28**, 48pp.

Wang, Y., 1998: On the bogusing of tropical cyclones in numerical models: The influence of vertical structure. *Meteorol. Atmos. Phys.*, **65**, 153-170.

Willoughby, H. E., 1995: Mature structure and evolution, Global Perspectives on Tropical Cyclones. *WMO Technical Document*, WMO/TD-No. 693, 21-62.

Zhang, D.-L., E.-Y. Hsie, and M. W. Moncrieff, 1988: A comparison of explicit and implicit predictions of convective and stratiform precipitating weather system with a meso-β scale numerical model. *Quart. J. Roy. Meteor. Soc.*, **114**, 31-60.

Zhang, D.-L., and R. A. Anthes, 1982: A high-resolution model of the planetary boundary layer-sensitivity tests and comparisons with SESAME-79 data. *J. Appl. Meteor.*, **21**, 1594-1609.

Zou, X., F. Vandenberghe, M. Pondeca, and Y.-H. Kuo, 1997: Introduction to Adjoint Techniques and the MM5 Adjoint Modeling System, *NCAR Tech. Note*, NCAR/TN-435-STR, 110pp.

Zou, X., and Q. Xiao, 1998: Initial structures within a mature hurricane vortex generated by a variational initialization scheme. *Preprints of 23rd Conference on Hurricane and Tropical Meteorology* (Vol. II), American Meteorology Society, 658-661.

Captions

Figure 1: Fran observed best track (hurricane symbol) starting from 0000 UTC 3 to 0600 UTC 6 September 1996 and model domains configuration. Domain A fixed, Domain B started at initial time and moved at 28h and 66h. Domain C started at 66h and moved at 70h, 74h.

Figure 2: The vortex specification relationship between ΔP and R for Hurricane Fran at 0000 UTC September 1996. The circle marked in the figure shows ΔP pertinent to the observed R.

Figure 3: Variations of different cost function terms with respect to iterations for B80 (the dot-dashed line for background term, dashed line for wind term and solid line for pressure term).

Figure 4: Cross-sections of a) temperature and b) specific humidity above hurricane Fran before variational initialization (CTL), and cross-sections of c) temperature (solid line) and temperature increments ΔT (^{o}C, shading), d) specific humidity (solid line) and its increments Δq_v (g/kg, shading) above hurricane Fran after initialization (B80), at time 0000 UTC 3 September 1996.

Figure 5: The predicted tracks of Hurricane Fran (1996) by CTL, B80, A80 and the observed best track from 0000 UTC 3 to 0600 UTC 6 September 1996. The predicted landing time is also indicated in the figure.

Figure 6: Variations of (a) hurricane central SLP (hPa) and (b) maximum low-level wind speed V_Max (m/s) predicted by CTL (dot-dashed), B80 (dashed), A80 (dotted) and the observed intensity (solid) from 0000 UTC 3 to 0600 UTC 6 September 1996.

Figure 7: Surface analyses of streamlines and isotachs (kt) using all the available data including the US Air Force reconnaissance and buoys and ships data at (a) 0100 UTC and (b) 0700 UTC 5 September 1996. The analyses are experimental research product of NOAA/ AMOL/HRD. The unit of wind speed in the figure is *kt* (1 *kt*=0.5166667 m/s).

Figure 8: Surface streamlines and isotachs (m/s, dashed lines) predicted by B80 at (a) 0100 UTC and (b) 0700 UTC 5 September 1996.

Figure 9: Cross-sections of a) temperature (unit: ^{o}C), b) specific humidity (unit: g/kg), c) horizontal wind speed (unit: m/s), and d) vertical velocity (dashline for descents and solid line for ascent, unit: cm/s) along AB in Fig. 8a, predicted by B80 at 49-h. Contour intervals for (a), (b), (c), and (d) are 2 ^{o}C, 2 g/kg, 5 m/s and 10 cm/s, respectively.

Figure 10: Radar reflectivity (dBZ) (a) predicted by B80 at 0000 UTC 6 September 1996 and (b)

captured at Wilmington, North Carolina, at 0028 UTC 6 September 1996.

Figure 11: The predicted tracks of Hurricane Fran (1996) by CTL, A80, A100, A140, A180, A220, A260 and the observed best track from 0000 UTC 3 to 0600 UTC 6 September 1996.

Figure 12: Hurricane intensity variations predicted by A80, A100, A140, A180, A220, A260 and the observation from 0000 UTC 3 to 0600 UTC 6 September 1996 for (a) hurricane central SLP (hPa) and (b) maximum low-level wind speed V_Max (m/s)

Figure 13: The SLP (hPa, dashed line), wind speed at 850 hPa (thick solid line) at initial time (0000 UTC 3 September 1996) for (a) A220V, (b) A220P and (c) CTL. Contour intervals for SLP and 850-hPa wind speed are 5 hPa and 5 m/s, respectively.

Figure 14: Variations of (a) hurricane central SLP (hPa) and (b) maximum low-level wind speed V_Max (m/s) predicted by CTL (dashed), A220P (dot-dashed), A220V (light dashed), A220 (dotted) and the observation (solid) from 0000 UTC 3 to 0600 UTC 6 September 1996.

Figure 15: Cross-sections of temperature (solid line) and temperature increments ΔT (°C, shading), along CD in figure 13 for (a) A220V and (c) A220P; and specific humidity (solid line) and its increments Δq_v (*g/kg*, shading) along CD in figure 13 for (b) A220V and (d) A220P, at time 0000 UTC 3 September 1996. Contour intervals for temperature and specific humidity are 2 °C and 2 g/kg, respectively. The shading scales for the increments are on the bottom of the figure.

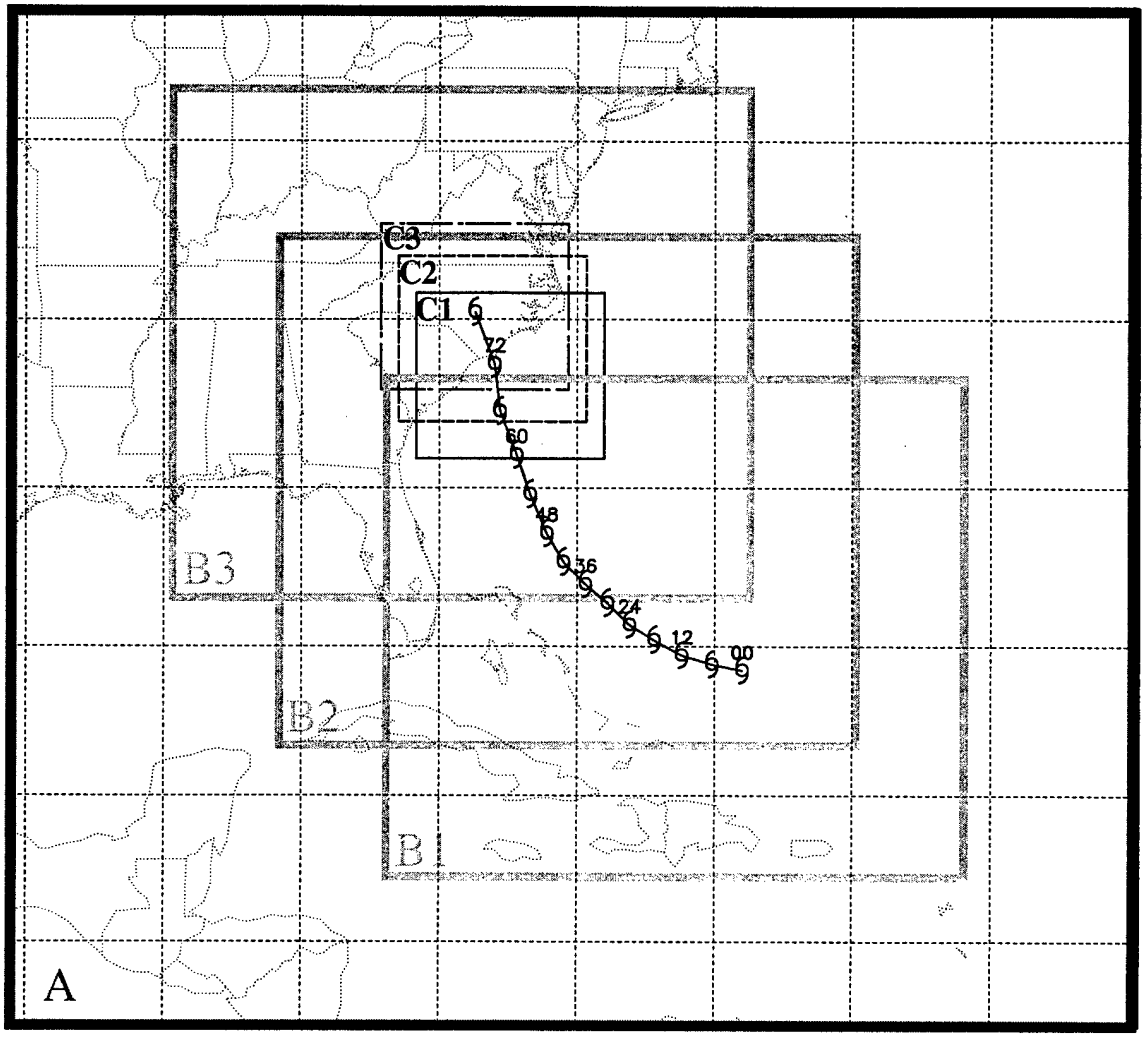

Fig. 1

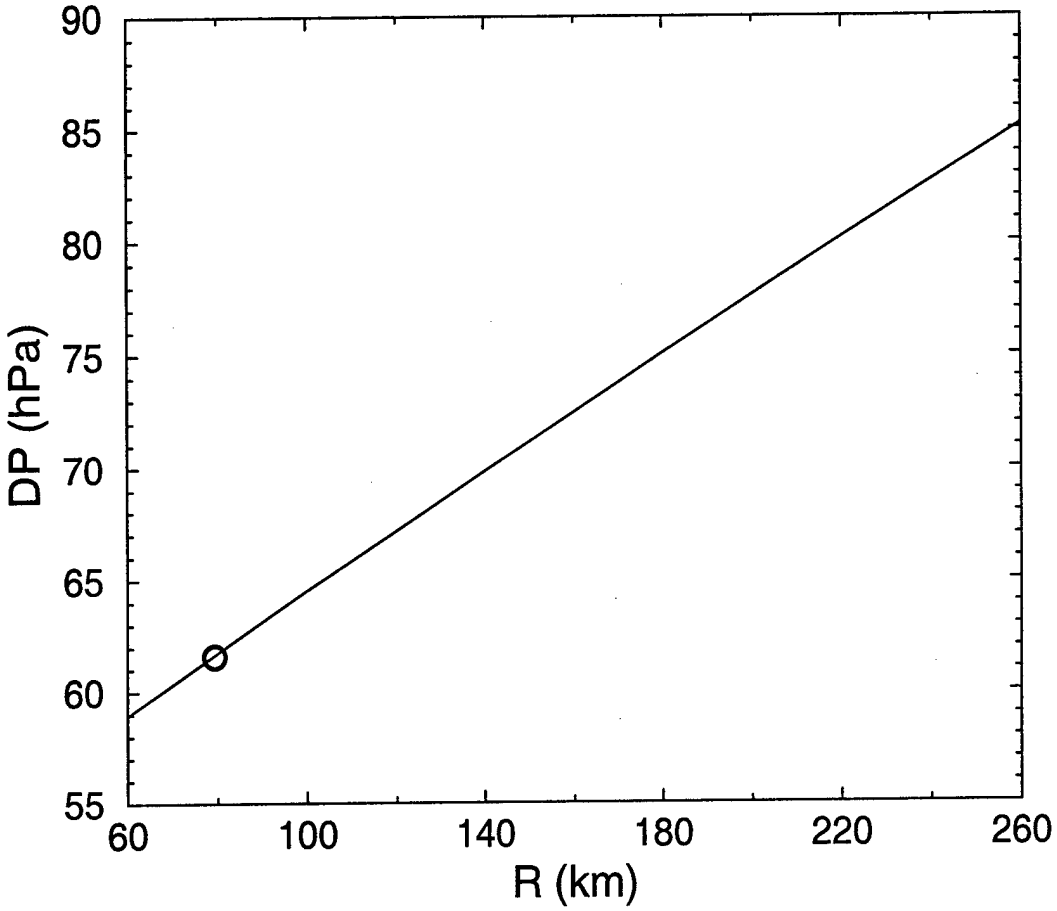

Fig. 2

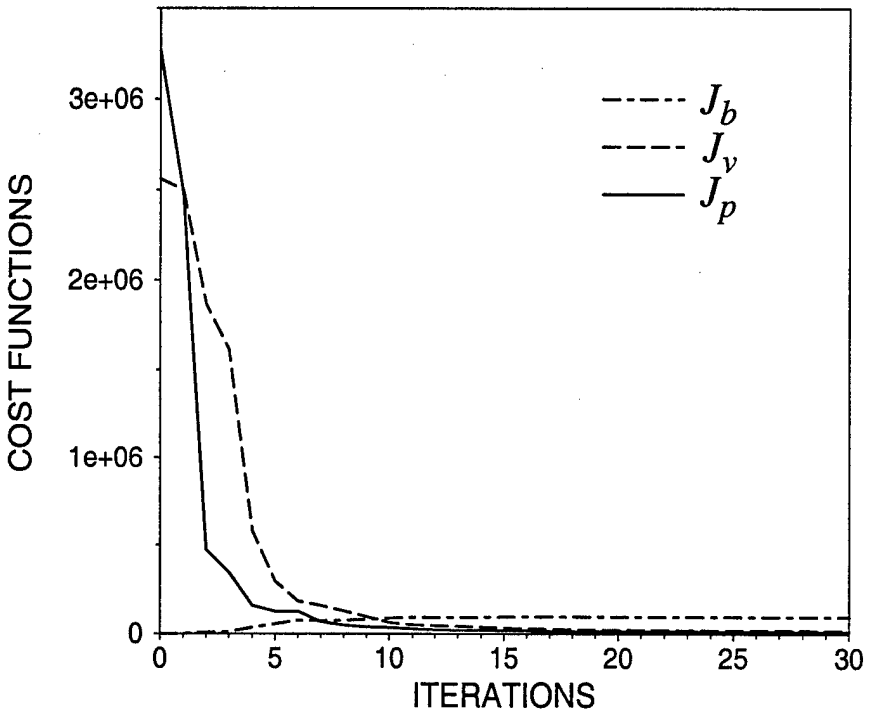
3e+06
2e+06
1e+06
0
COST FUNCTIONS
0
5
10
15
20
25
30
ITERATIONS
J_b
J_v
J_p

Fig. 3

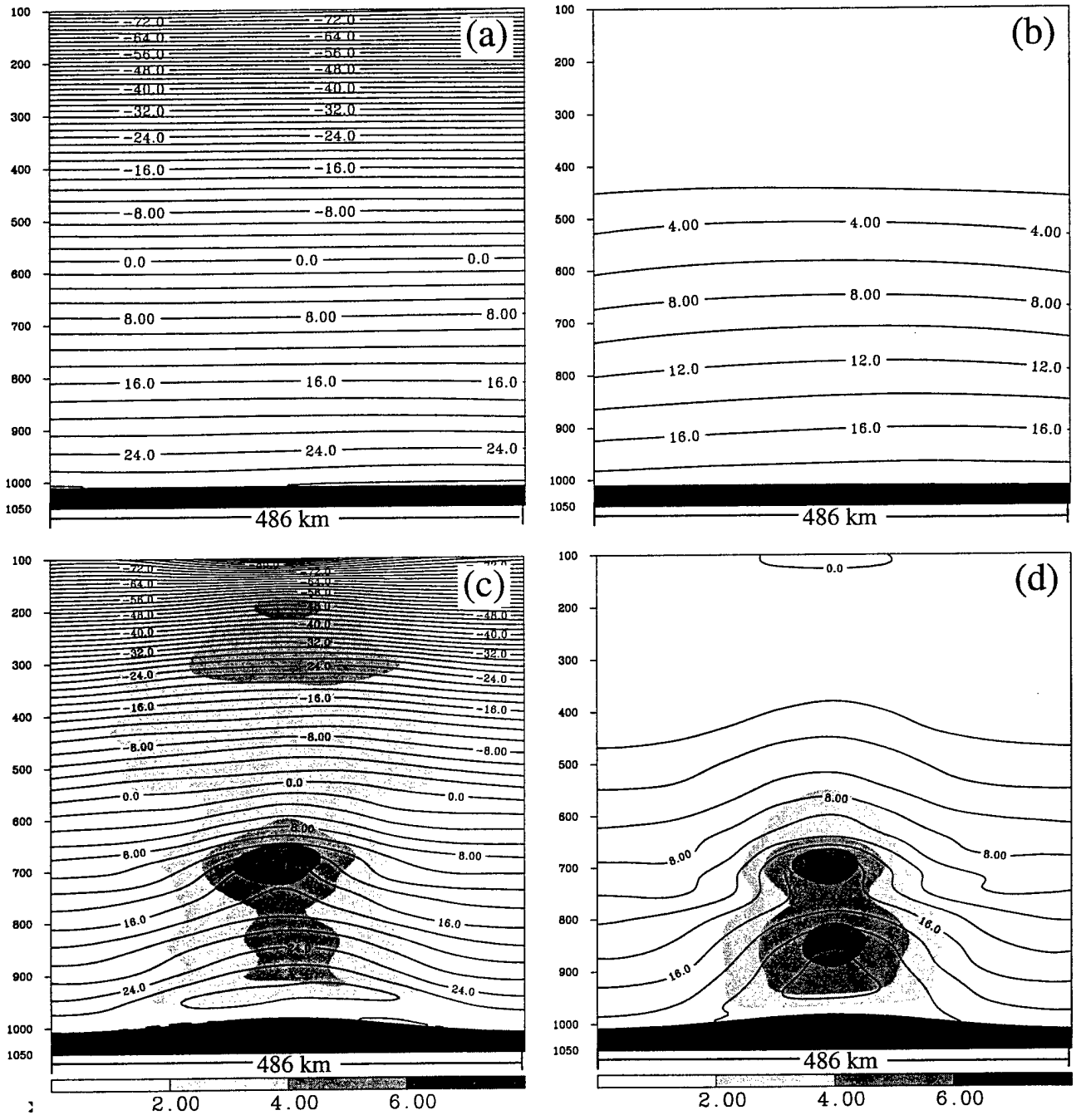

Fig. 4

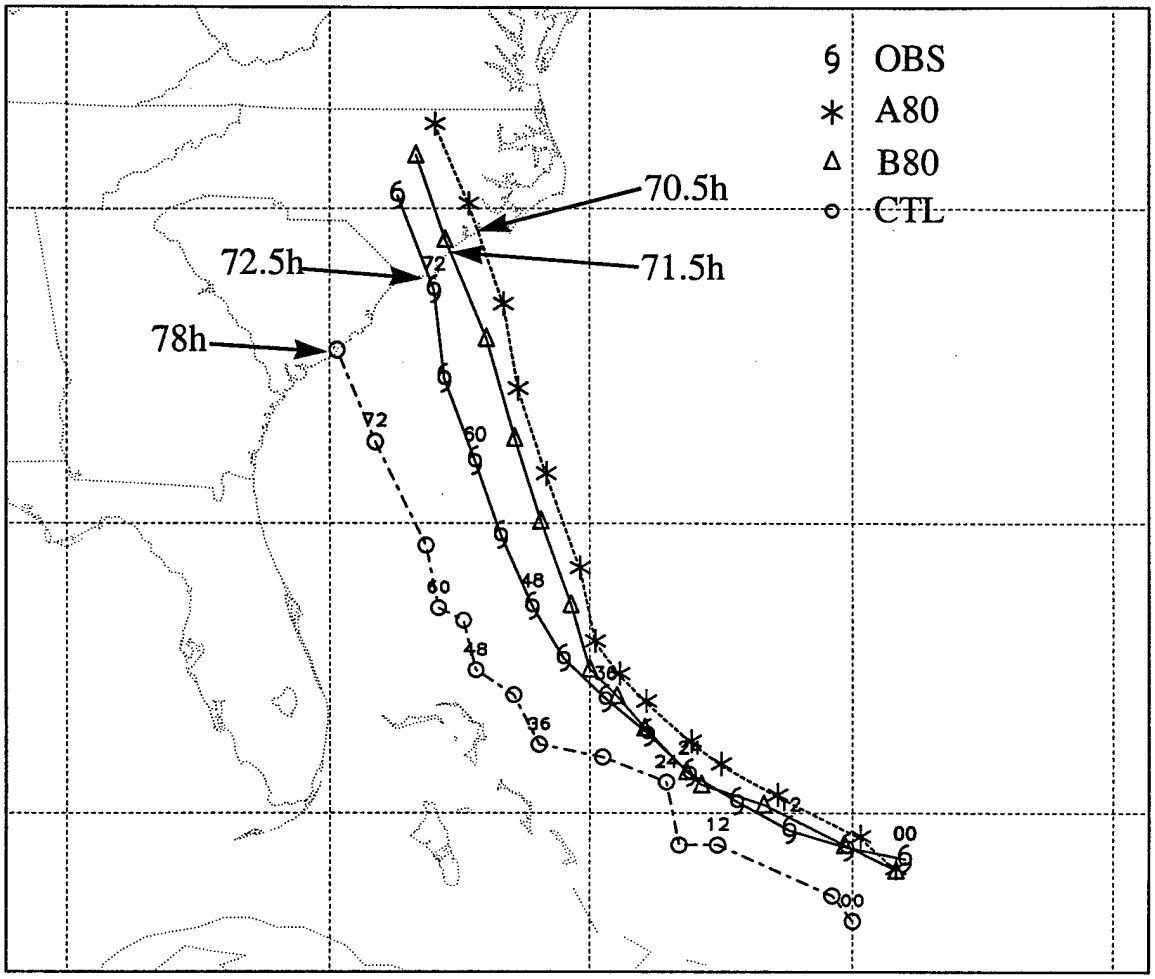

Fig. 5

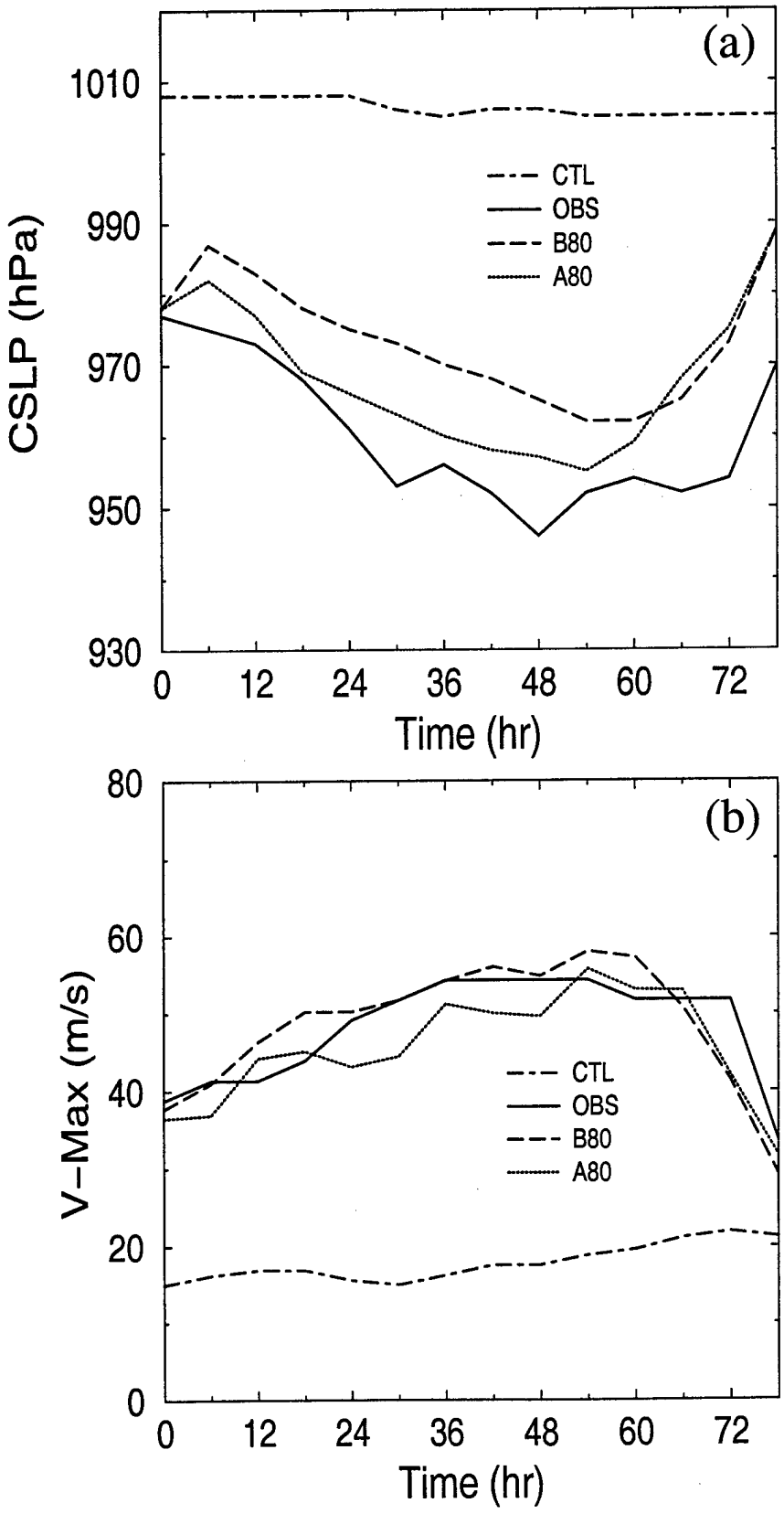
(a)
1010
990
970
950
930
CSLP (hPa)
CTL
OBS
B80
A80
0
12
24
36
48
60
72
Time (hr)
(b)
80
60
40
20
0
V–Max (m/s)
CTL
OBS
B80
A80
0
12
24
36
48
60
72
Time (hr)

Fig. 6

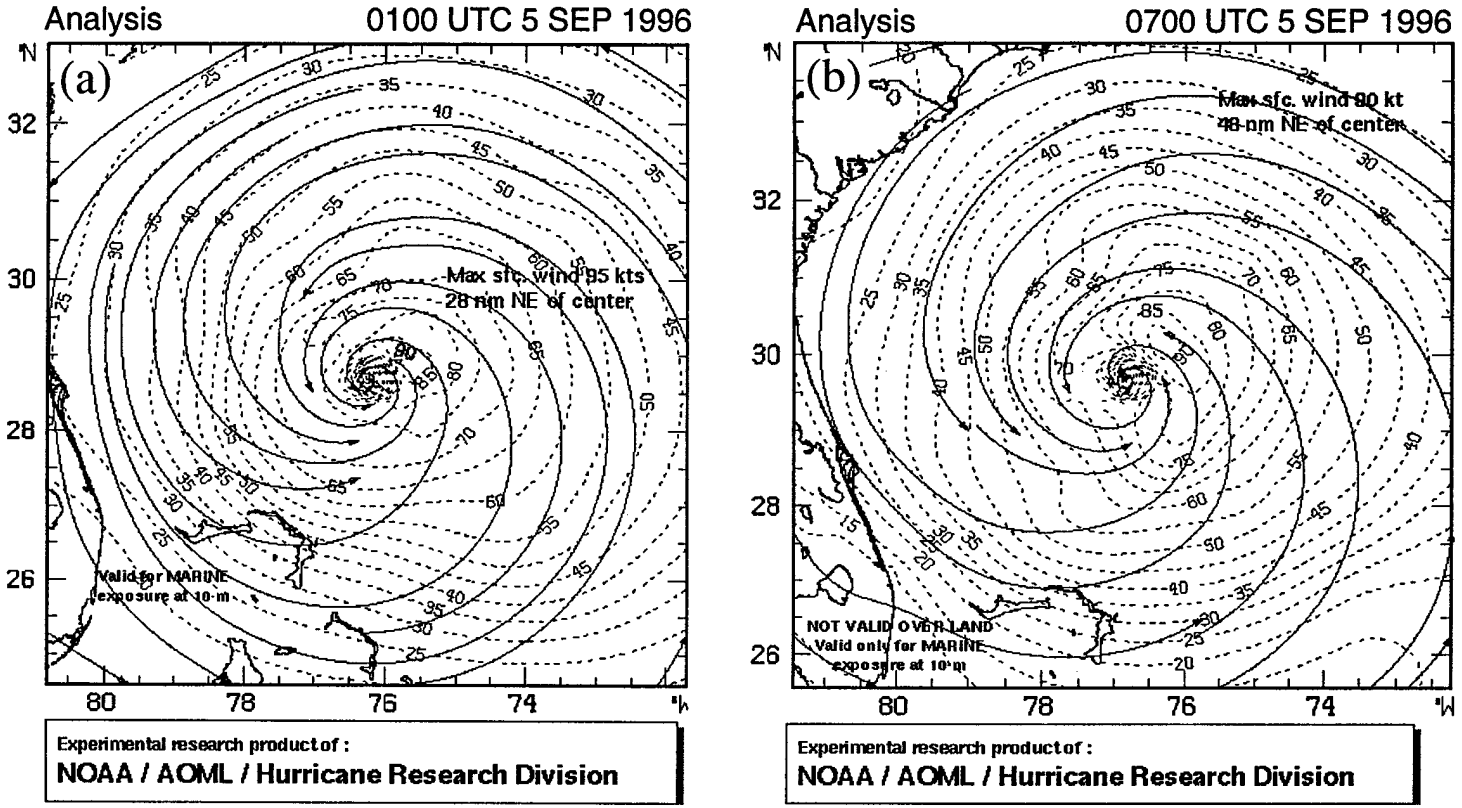
Analysis
0100 UTC 5 SEP 1996
(a)
Max sfc. wind 95 kts
28 nm NE of center
Valid for MARINE
exposure at 10-m
Experimental research product of :
NOAA / AOML / Hurricane Research Division
Analysis
0700 UTC 5 SEP 1996
(b)
Max sfc. wind 80 kt
48 nm NE of center
NOT VALID OVER LAND
Valid only for MARINE
exposure at 10-m
Experimental research product of :
NOAA / AOML / Hurricane Research Division

Fig. 7

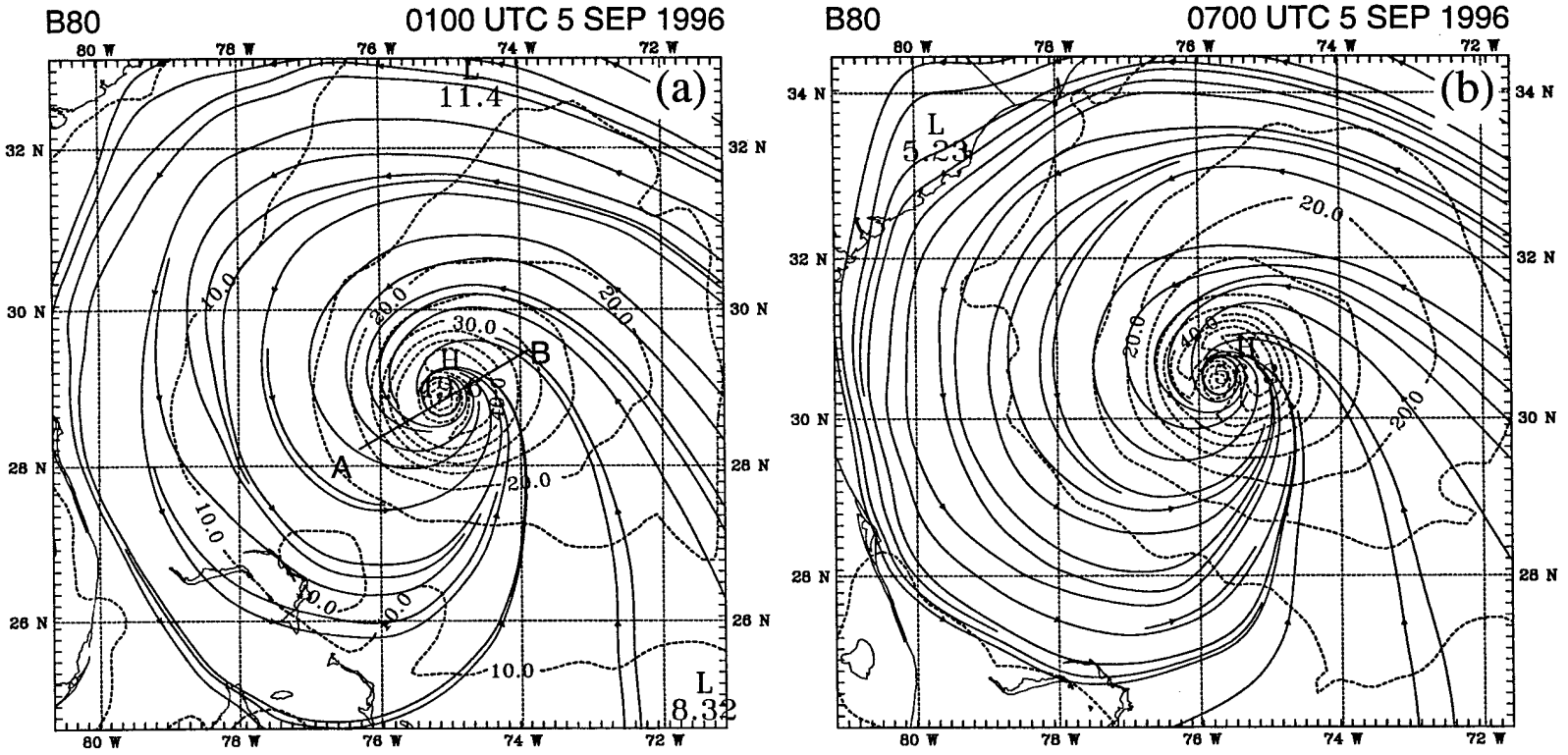
B80
0100 UTC 5 SEP 1996
(a)
L
11.4
H
B
A
L
8.32
B80
0700 UTC 5 SEP 1996
(b)
L
5.23
80 W
78 W
76 W
74 W
72 W
34 N
32 N
30 N
28 N
26 N
10.0
20.0
30.0

Fig. 8

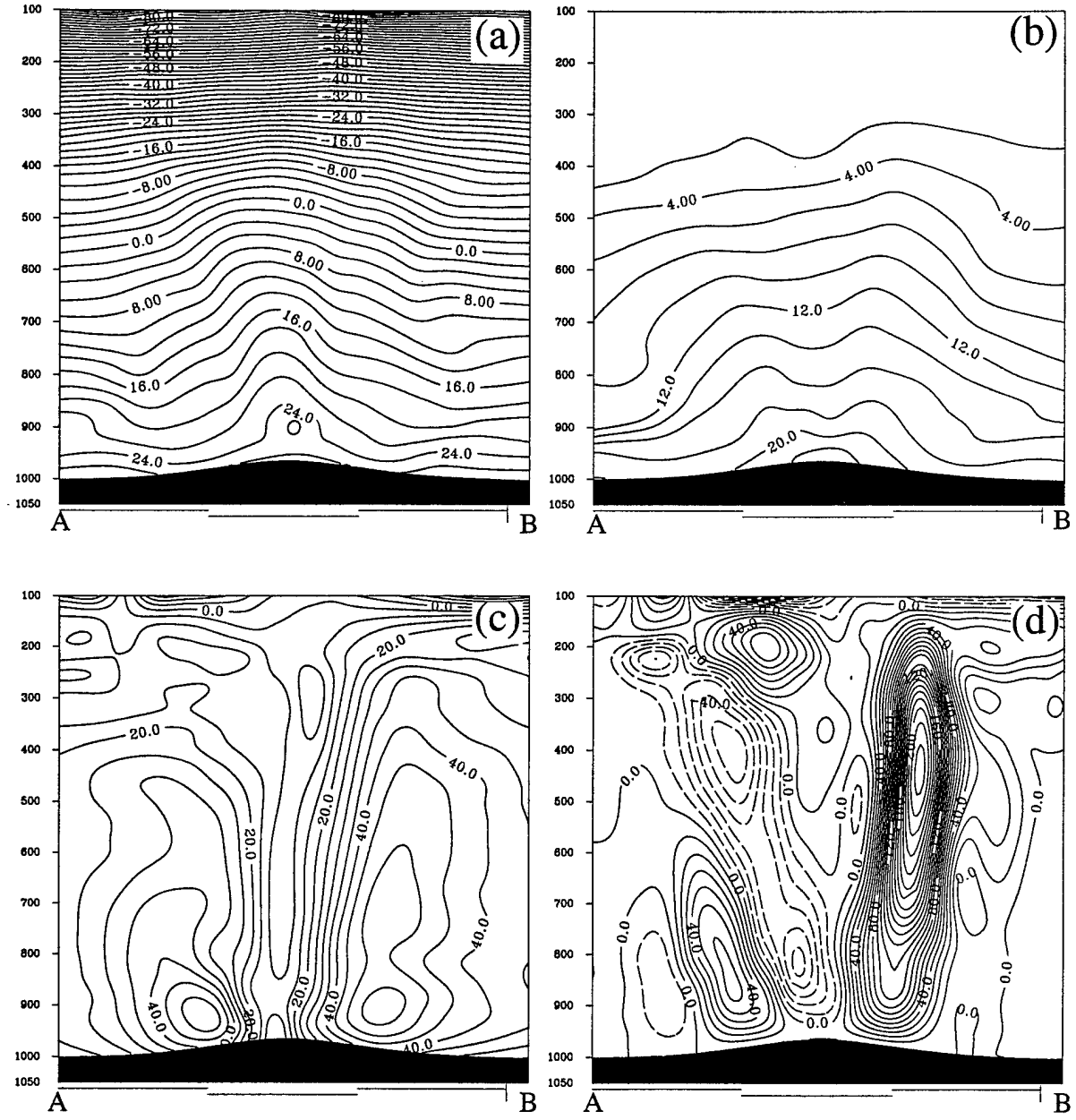

Fig. 9

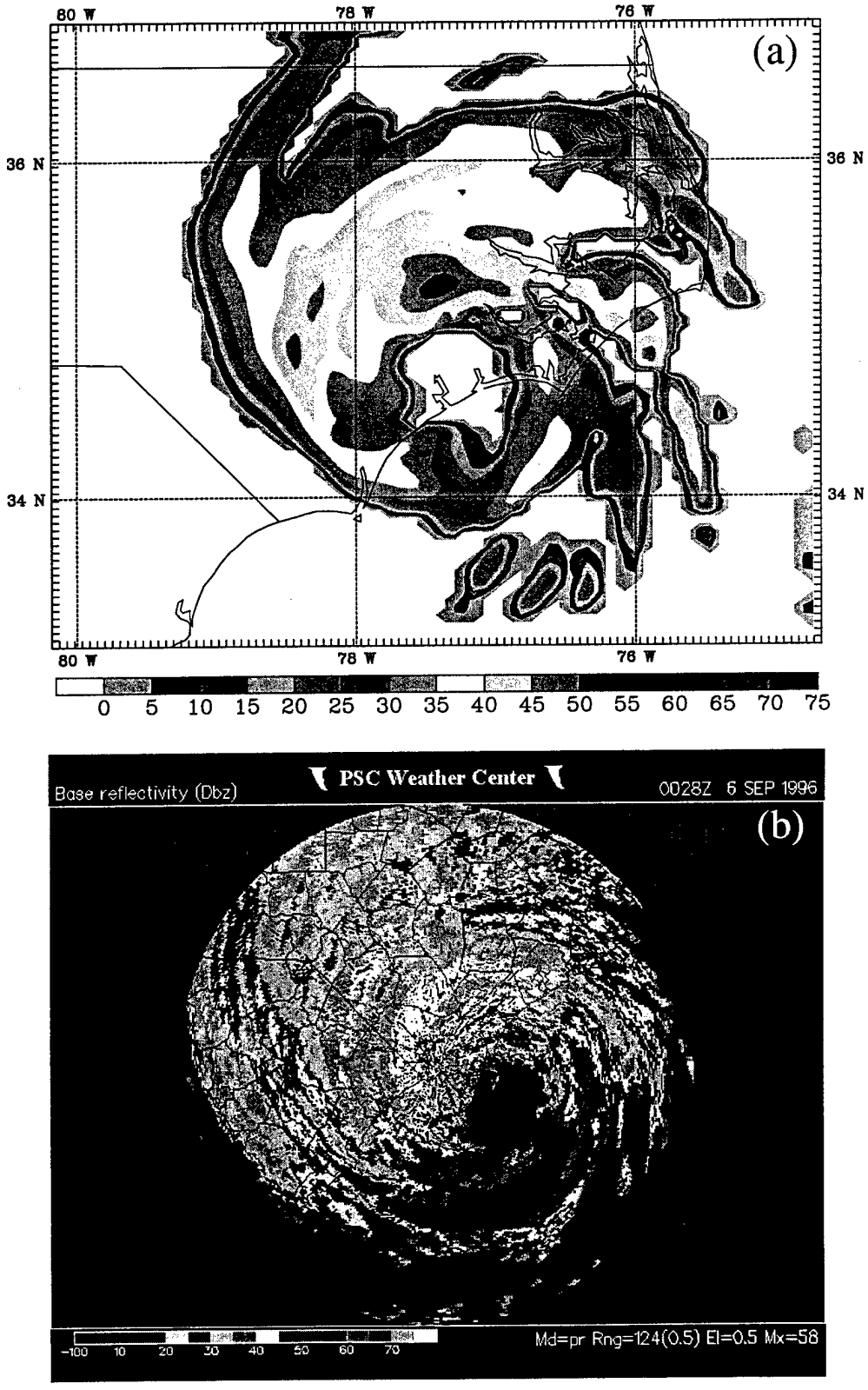
80 W
78 W
76 W
(a)
36 N
34 N
0 5 10 15 20 25 30 35 40 45 50 55 60 65 70 75
Base reflectivity (Dbz)
PSC Weather Center
0028Z 6 SEP 1996
(b)
Md=pr Rng=124(0.5) El=0.5 Mx=58

Fig. 10

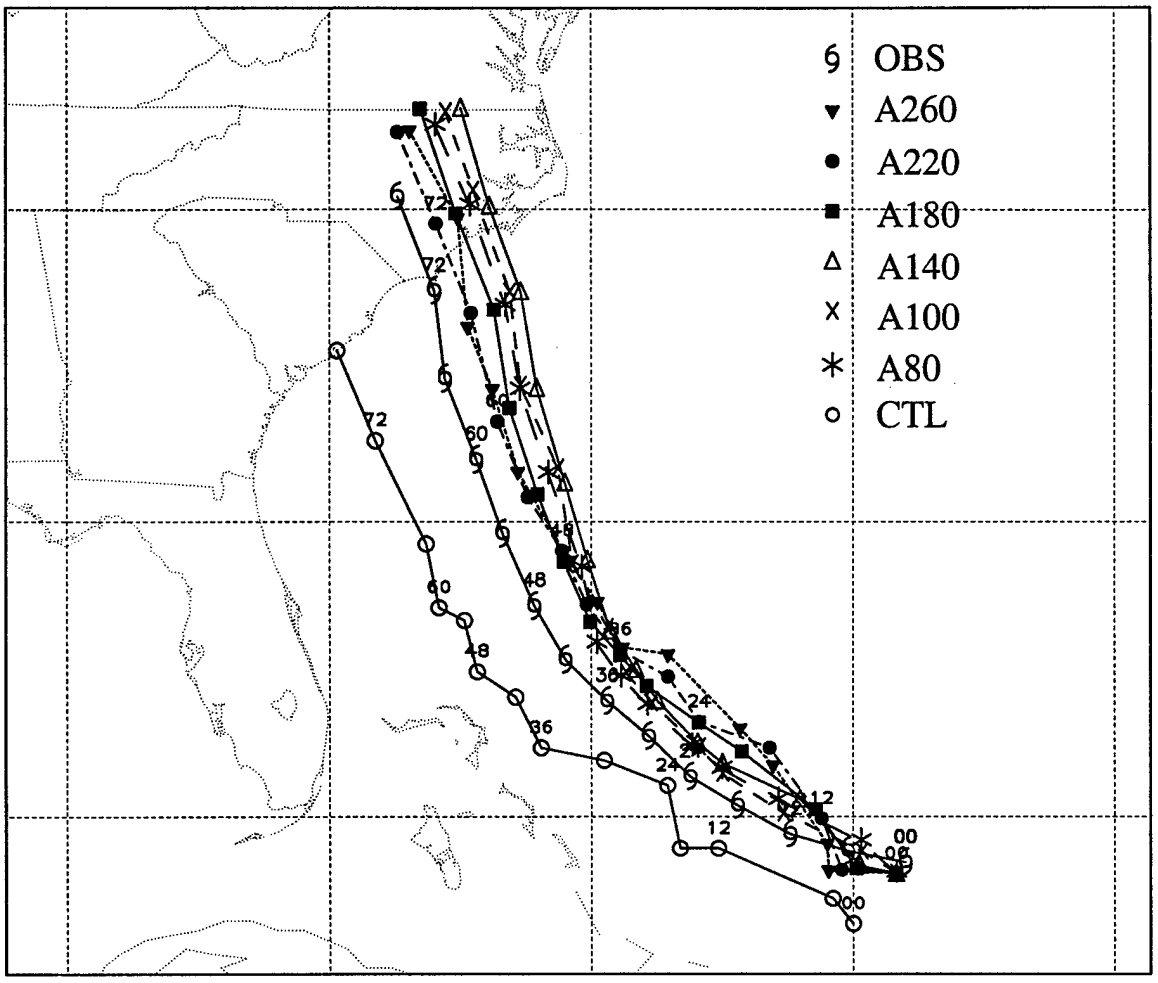

Fig. 11

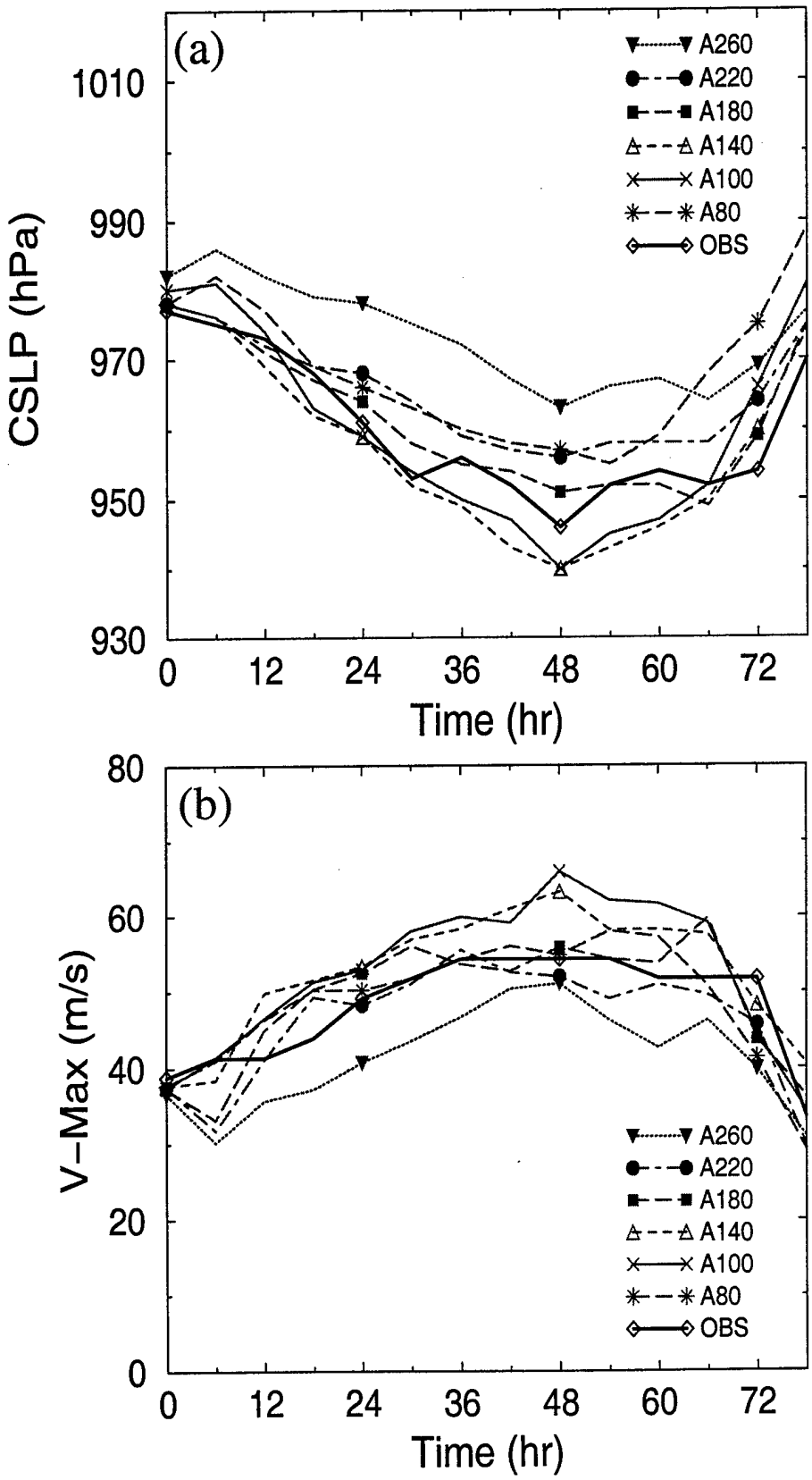
(a)
1010
990
970
950
930
CSLP (hPa)
0
12
24
36
48
60
72
Time (hr)
A260
A220
A180
A140
A100
A80
OBS
(b)
80
60
40
20
0
V-Max (m/s)
0
12
24
36
48
60
72
Time (hr)
A260
A220
A180
A140
A100
A80
OBS

Fig. 12

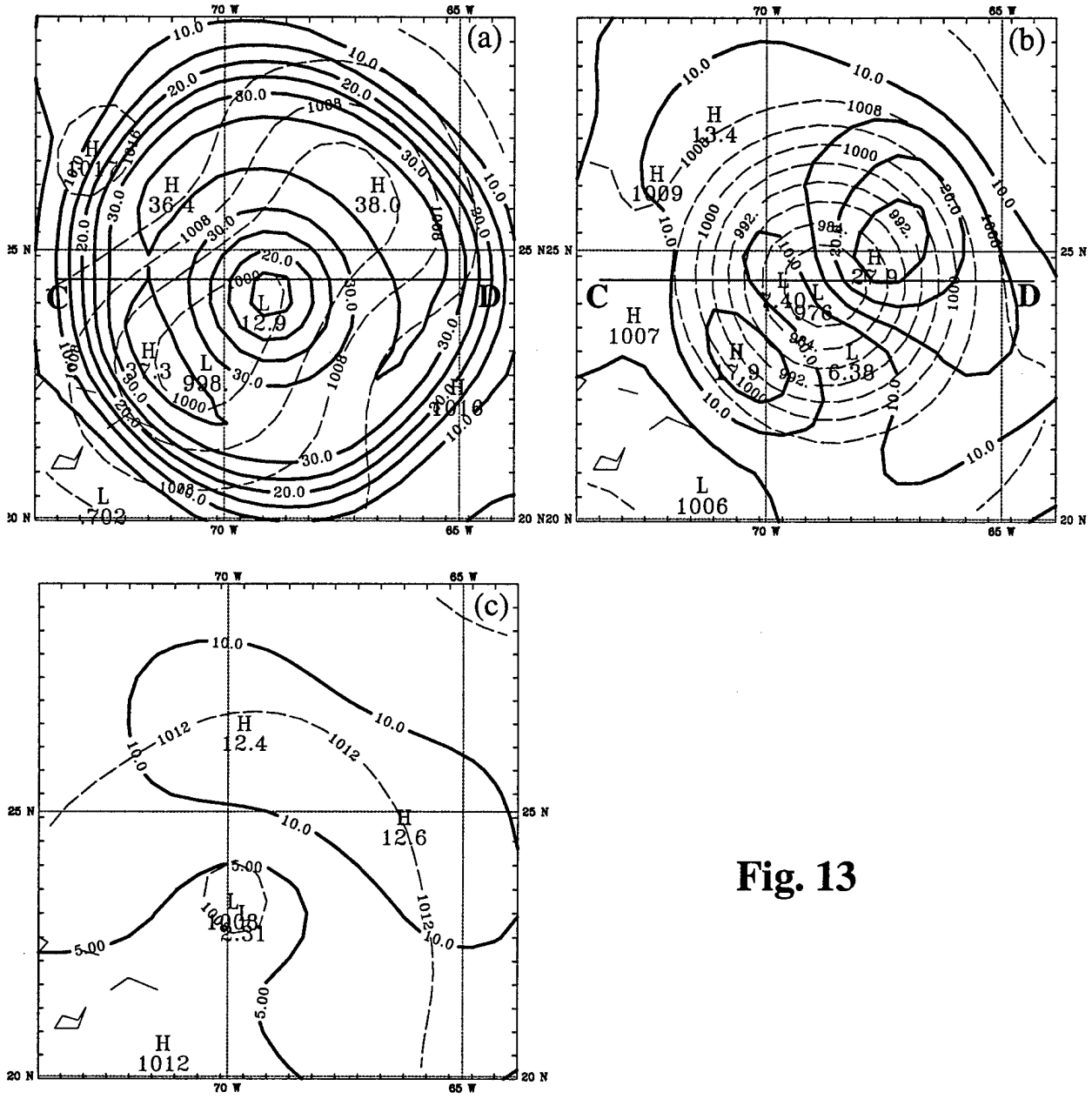

Fig. 13

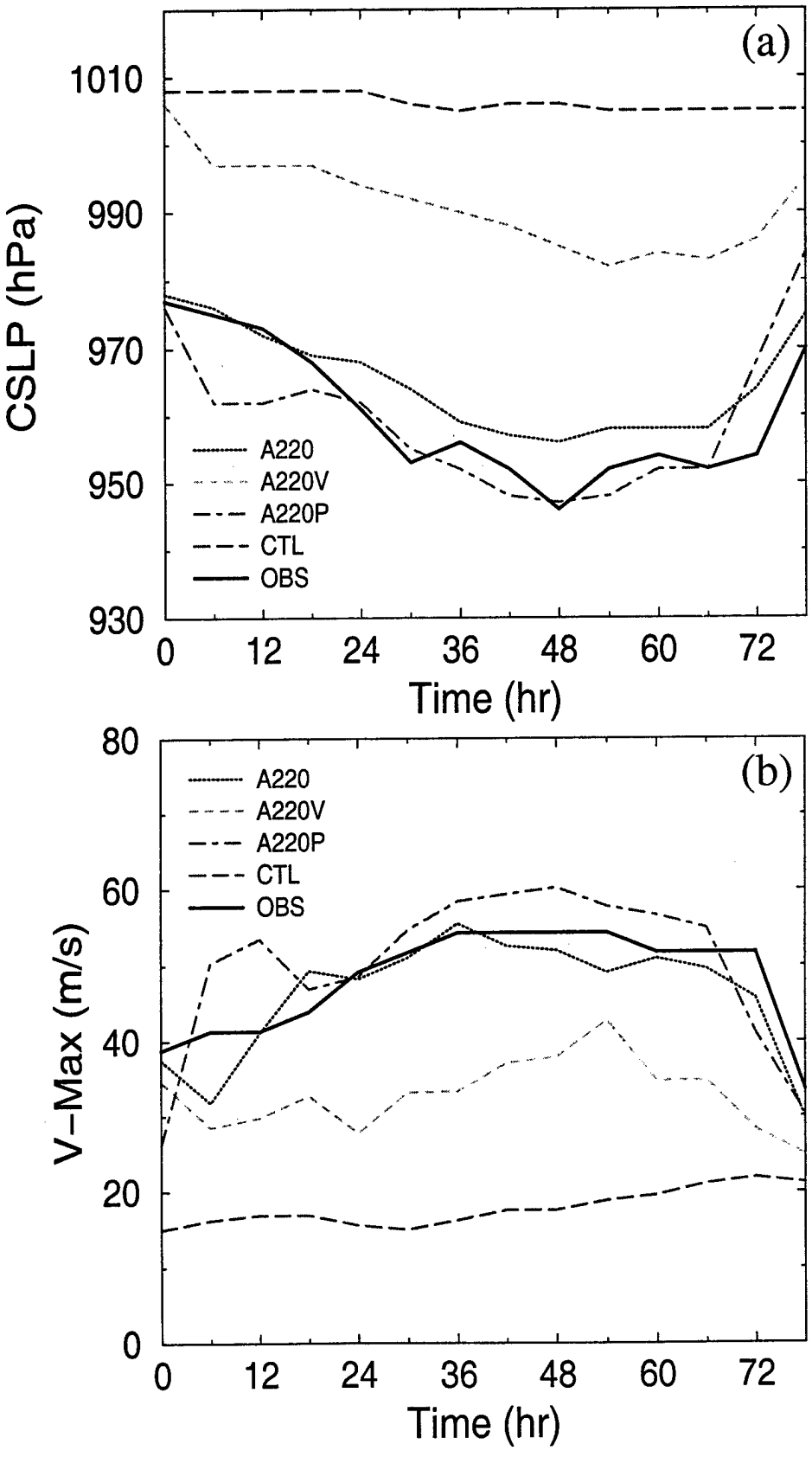
(a)
1010
990
970
950
930
CSLP (hPa)
A220
A220V
A220P
CTL
OBS
0
12
24
36
48
60
72
Time (hr)
(b)
80
60
40
20
0
V–Max (m/s)
A220
A220V
A220P
CTL
OBS
0
12
24
36
48
60
72
Time (hr)

Fig. 14

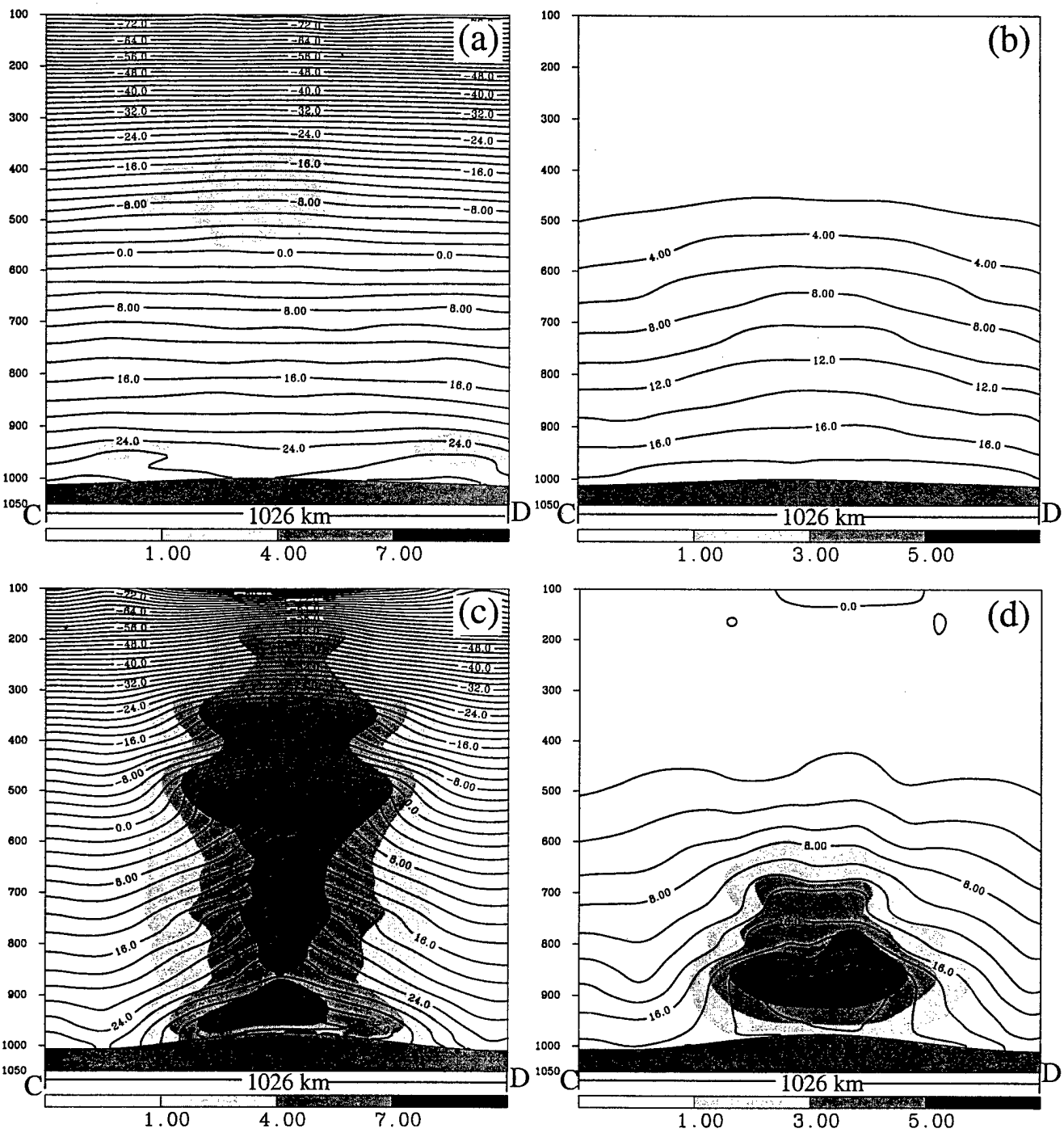

Fig. 15